JETP Letters, Vol. 73, No. 1, 2001, pp. 6–9. Translated from Pis'ma v Zhurnal Éksperimental'noĭ i Teoreticheskoĭ Fiziki, Vol. 73, No. 1, 2001, pp. 8–12.

Giant Second Harmonic Generation in Microcavities Based on Porous Silicon Photonic Crystals

T. V. Dolgova[1], A. I. Maĭdikovskiĭ[1], M. G. Martem'yanov[1], G. Marovsky[2], G. Mattei[3], D. Schuhmacher[2], V. A. Yakovlev[4], A. A. Fedyanin[1], and O. A. Aktsipetrov[1,*]

[1] Moscow State University, Vorob'evy gory, Moscow, 119899 Russia

** e-mail: aktsip@shg.phys.msu.su*

[2] Laser-Laboratorium Göttingen, D-37077 Göttingen, Germany

[3] Instituto di Metodologie Avanzate Inorganiche, CNR, Monterotondo Scalo 00016, Italy

[4] Institute of Spectroscopy, Russian Academy of Sciences, Troitsk, Moscow region, 142092 Russia

Received November 28, 2000

The experimental spectral dependence of the intensity of the second harmonic (SH) generated in microcavities based on porous silicon photonic crystal demonstrates resonant intensity enhancement (by a factor of $\sim 2 \times 10^2$) in the vicinity of the cavity mode and at the edges of the photonic band gap. The enhancement is due to the combined effect of pump radiation localization inside the microcavity, multiple SH interference in the photonic crystal, and two-photon resonance of the porous silicon quadratic susceptibility at the SH frequency.

PACS numbers: 42.65.Ky; 42.70.Qs

Photonic crystals (PCs) are the microstructures with periodically modulated optical (including high-order) susceptibility with a period on the order of the optical wavelength. They possess unique physical properties and are of great practical interest. The presence of a photonic band gap, i.e., the range of optical frequencies where the electromagnetic field exponentially decays inside the PC, renders them candidates for use in optical switches and optical transistors [1], as well as in PC lasers with extremely low lasing threshold [2]. PCs exhibit unique optical effects such as giant optical dispersion [3], optical bistability [4], and light localization [5]. So far, most attention in studying the nonlinear optical properties of PCs has been given to efficient frequency doubling, because the conditions for quasi-phase-matching are fulfilled in PCs. Quasi-matching can be attained (1) in nonlinear PCs with quadratic susceptibility periodically modulated in one or two directions and uniform linear susceptibility [6] and (2) in PCs with modulated linear susceptibility [7, 8]. In the latter case, the quasi-matching condition can be fulfilled if either the pump frequency or the second harmonic (SH) frequency falls on the edge of the photonic band gap in the PC. Naturally, such PCs were fabricated from noncentrosymmetric materials with large bulk quadratic susceptibility: lithium niobate [6], gallium arsenide [7], and zinc sulfide [8]. Of particular interest is the investigation of the nonlinear optical response of a PC fabricated from centrosymmetric materials, e.g., porous silicon (PS) [9]. Porous silicon PCs are grown using a comparatively simple electrochemical technique that provides high reproducibility of parameters. This method has become part of modern silicon technology, thereby resulting in the high practical importance of porous silicon PCs and microstructures on their base. It is of interest to explore the nonlocal effects in the nonlinear optical response of PC-based microcavities (MCs). The parameters of the distributed PC mirrors of such Fabry–Pérot microcavities determine the MC *Q* factor. This permits the control of the electromagnetic field localization in the MC at the frequency of the cavity mode, providing enhancement of the MC optical response, e.g., luminescence [10] and Raman scattering [11]. The MC mode within the photonic band gap is analogous to the impurity level within the semiconductor electronic energy gap. The spectral position of the cavity mode in the photonic band gap can be changed by varying the MC parameters [layer thicknesses in PC mirrors and the MC ("impurity") level], allowing the control of the enhancement effects in the nonlocal nonlinear MC optical response.

This work reports the experimental results on the intensity spectrum of the SH generated in porous silicon microcavities. The enhancement of the SH response was observed in the vicinity of the cavity mode and at the edges of the photonic band gap. The SH generation in a multilayer structure with distributed nonlinear sources is phenomenologically described with account taken of the multiple interference of the pump and SH fields. It is shown that the enhancement of SH response at the frequency of the MC mode differs in nature from the enhancement at the edges of the photonic band gap: the mode SH resonance is caused by the

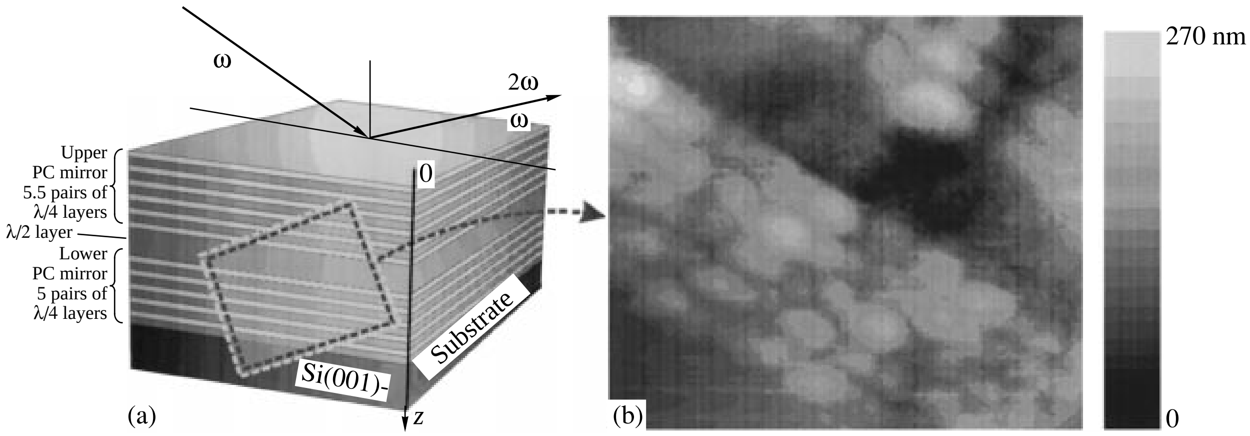

Fig. 1. Left: porous silicon MC structure and geometry of the experiment; light regions correspond to the optically denser PS layers. Right: MC cut image obtained on a scanning microscope with a quasi-friction detector. The gray scale of the displacement of the tip with respect to the MC cleavage face at a constant friction force is given on the right.

localization (amplification) of the standing pump wave in the vicinity of the MC layer, whereas the SH resonance at the edge of the photonic band gap is caused by a uniform amplification of the pump field in the distributed PC mirrors of the microcavity.

Microcavity samples (Fig. 1a) were composed of two one-dimensional PCs formed by five pairs of quarter-wave (λ_0 = 945 nm) PS layers and a half-wave PS cavity layer as a spacer. The samples were prepared by electrochemical etching [12] of a single-crystal *p*-type silicon wafer in the crystallographic (001) orientation with a resistivity of 0.01 Ω cm in an electrolyte consisting of a 50% solution of hydrofluoric acid and ethyl alcohol taken in 1 : 2 v/v ratio. The alternating PS layers of different porosity (air volume concentration) were obtained by periodic modulation of the current density flowing through the silicon wafer perpendicularly to its surface. The etching rate was determined by the current density of the electrochemical process and the resistivity of the silicon wafer. The porosities and thicknesses were, respectively, f_h = 0.77 and d_h = 160 nm for the optically denser PC layers and f_l = 0.88 and d_l = 200 nm for the less dense layers. The cavity layer was formed from PS with f_r = 0.88 and d_r = 400 nm. Figure 1b is the MC cut image obtained on a scanning force microscope with a piezoelectric quasi-friction force detector based on a 32.8-kHz quartz tuning-fork. The scanning tip was made from a single-mode fiber by etching in a protective envelope. Light areas in the image correspond to a high longitudinal friction, i.e., to the less porous regions. The strict periodicity in the PS layers and the 5-μm-scale longitudinal homogeneity of the structure confirm the high quality of the prepared samples. However, it was hard to determine the thickness ratio for the PS layers of different porosity because the scanning tip had a large radius (on the order of 50 nm) of curvature, resulting in an asymmetry toward the denser PS layers.

The SH spectra were recorded using a Spectra-Physics MOPO 710 optical parametric oscillator (OPO), tuned in the range 730–1100 nm, with a 10-ns pulse duration and pulse energy of approximately 10 mJ, excited by the third harmonic of a YAG laser. Collinear phase matching in the OPO nonlinear crystal provided a fixed angle of incidence θ for the pump radiation upon frequency tuning. The SH radiation from the MC sample was filtered and focused onto the photomultiplier cathode. To normalize the SH spectrum to the frequency-dependent photomultiplier sensitivity and filter transmission coefficients, a portion of the pump radiation was fed into the reference channel that was identical to the main channel and contained *z*-quartz crystal as a source of calibrating SH radiation. For linear spectroscopy, the pump radiation reflected from the MC sample was detected by a photodiode and normalized to the intensity of incident light.

For the *p*- and *s*-polarized pump radiations (*p*–*p* and *s*–*p* geometries, respectively), the intensity of the *p*-polarized SH radiation reflected from the MC was independent of the angle of rotation of the MC sample about its normal, to within the experimental error caused by a weak inhomogeneity of the MC in its plane.

The dependence of the SH intensity $I_{2\omega}$ on the pump wavelength λ_ω, measured for the angle of incidence θ = 45° in the *s*–*p* geometry, is shown in Fig. 2a. For comparison, the spectrum of the linear reflection coefficient (R_s) of the *s*-polarized pump radiation is presented in Fig. 2d. In the vicinity of 780 nm, corresponding to the spectral position of the MC mode, $I_{2\omega}$ increases by a factor of ~2×10^2, as compared to the SH intensity in the band gap. Another resonance feature is observed in the vicinity of 910 nm (~50-fold enhancement), which coincides with the long-wavelength edge of the photonic band gap. The increase in the SH intensity at the short wavelength edge of the photonic band gap is much

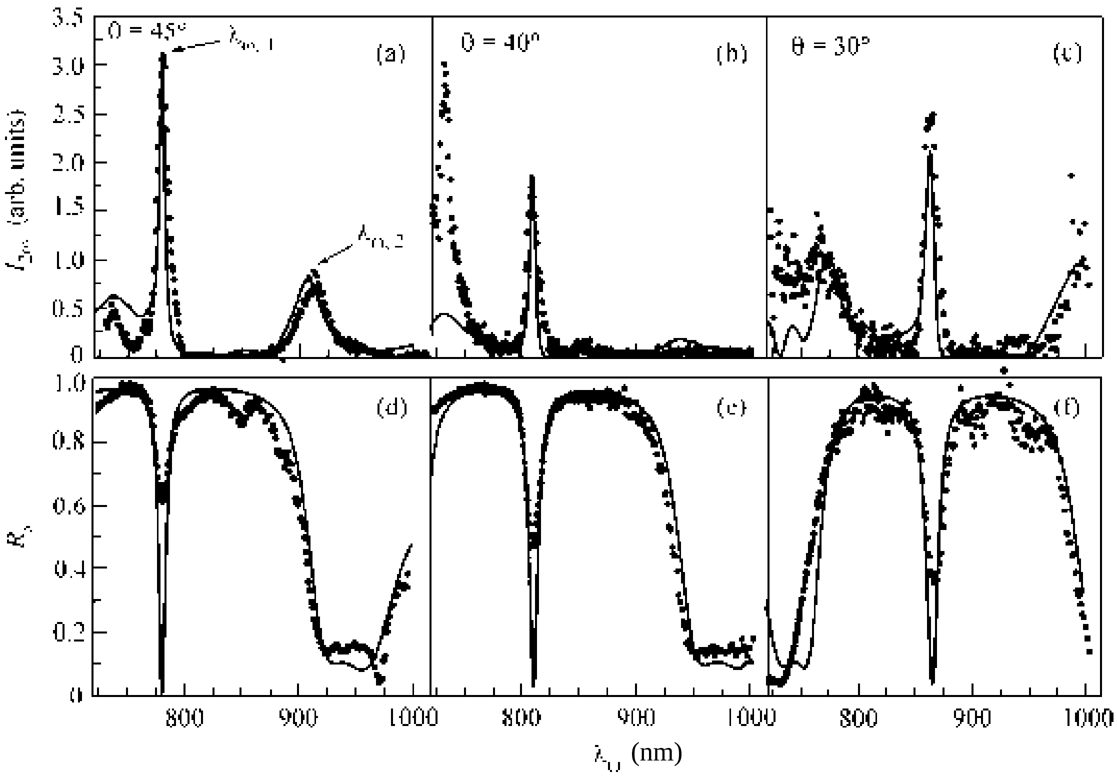

Fig. 2. Intensity of the *p*-polarized SH radiation as a function of the wavelength of *s*-polarized pump radiation, measured in the porous silicon MC at different angles of incidence: θ = (a) 45°, (b) 40°, and (c) 30°. The SH intensities in panels (b) and (c) are given on 7- and 20-fold enlarged scales, respectively. Solid lines are the results of model calculations. Reflectivity spectra are given for the *s*-polarized pump radiation at different angles of incidence: θ = (d) 45°, (e) 40°, and (f) 30°.

smaller. When changing θ to 40° (Fig. 2b) and 30° (Fig. 2c), the SH resonances are shifted to longer wavelengths. This correlates with the angular dependence of the cavity mode in the $R_s(\lambda_\omega)$ spectra (Figs. 2e, 2f). The greatest SH enhancement at the edge of the photonic band gap ($\sim 1 \times 10^2$) is observed at θ = 55° (Fig. 3a).

The spectrum of the SH radiation reflected from the PS microcavity was calculated by using the following phenomenological approach. At the first step, the transfer-matrix formalism was used to solve the problem of multiple interference of pump radiation in a multilayer structure with the dispersion $\varepsilon_{PS}(\lambda)$ calculated for each PS layer in the effective-medium approximation [13] taking the dispersion $\varepsilon_{Si}(\lambda)$ of single-crystal silicon as a basis [14]:

$$(1-f)\frac{\varepsilon_{Si}-\varepsilon_{PS}}{\varepsilon_{Si}+2\varepsilon_{PS}} = f\frac{\varepsilon_{PS}-1}{1+2\varepsilon_{PS}}. \qquad (1)$$

This was used to calculate the reflection coefficient $R_{s(p)}$ of the polarized pump radiation and the spatial distribution of the amplitude $\mathbf{E}_\omega^{(j)}(z) = \mathbf{E}_\omega^{+(j)}\exp(ik_{\omega,z}^{(j)}z) + \mathbf{E}_\omega^{-(j)}\exp(-ik_{\omega,z}^{(j)}z)$ of the pump standing wave inside the *j*th layer of the microcavity. At the second step, the components of quadratic polarization were calculated for each layer to determine the coupled SH wave field. It was assumed that the quadratic susceptibility $\chi^{(2)(j)}$ is uniformly distributed inside the *j*th layer and that only the $\chi_{zxx}^{(2)(j)} = \chi_{zyy}^{(2)(j)}$ components are involved in the SH generation by the *s*-polarized pump radiation (the point group of the PS layer was assumed to be ∞m). The spectral behavior of the effective components of quadratic susceptibility was modeled for the *j*th layer by the sum of two Lorentzians, $\chi^{(2)(j)}(2\omega) = (a - b_1/(-\Omega_1 + 2\omega + i\Gamma_1) - b_2/(-\Omega_2 + 2\omega + i\Gamma_2))f_j^{-2}$, with $\hbar\Omega_1$ = 3.36 eV and $\hbar\Omega_2$ = 4.3 eV corresponding to the direct electronic transitions E_0'/E_1 and E_2 in silicon [14]. Next, the nonlinear transfer-matrix formalism, analogous to that applied in [15] to the generation of the third harmonic, was used to solve the problem of interference of the coupled and free SH waves in the *j*th layer and the problem of linear propagation of the SH wave in the structure with multiple interference. The SH amplitude from the whole microcavity was found by summing the SH fields from each of the layers.

The calculated SH and linear reflection spectra are shown in Figs. 2 and 3a by solid lines to demonstrate good qualitative agreement with the experiment. The calculations were carried out for all angles of incidence and the following MC parameters: thicknesses d_l =

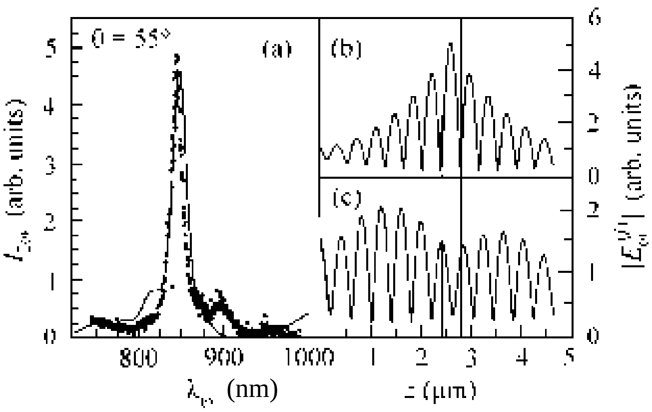

Fig. 3. (a) Intensity of the *p*-polarized SH radiation as a function of the wavelength of *s*-polarized pump radiation, measured in the porous silicon MC at θ = 55°. Solid line is the result of model calculations. (b) Spatial distribution of the pump standing wave amplitude in the MC, calculated for the wavelength $\lambda_{\omega,1}$ = 781 nm corresponding to the microcavity mode at θ = 45°, and (c) $\lambda_{\omega,2}$ = 909 nm corresponding to the edge of the photonic band gap. Vertical lines indicate the boundaries of the cavity layer.

204 nm, d_h = 165 nm, and d_r = 408 nm and porosities f_h = 0.774 and $f_l = f_r$ = 0.882. Figures 3b and 3c show the spatial distribution of the absolute value of local amplitude $|\mathbf{E}_\omega^{(j)}(z)|$ of the pump standing wave in the MC at two characteristic wavelengths: $\lambda_{\omega,1}$ = 781 nm (corresponding to the MC mode) and $\lambda_{\omega,2}$ = 909 nm (coinciding with the SH maximum at the long-wavelength edge of the photonic band gap). In the vicinity of $\lambda_{\omega,1}$, the pump field is mostly localized in the microcavity and the volume energy density of pump radiation exponentially decreases as the outer edges of the PC mirrors are approached. At the wavelength $\lambda_{\omega,2}$, the pump field is amplified uniformly throughout the MC. Since the induced quadratic polarization is $\mathbf{P}_{2\omega}^{(2)(j)}(z) \propto \mathbf{E}_\omega^{(j)}(z)\mathbf{E}_\omega^{(j)*}(z)$, the resonance enhancement of the SH signal in the vicinity of $\lambda_{\omega,1}$ is caused by the effects of pump field localization in the MC layer and the adjacent layers of the PC mirrors. Note that, due to the half-wave thickness of the MC layer, its contribution to the SH at $\lambda_{\omega,1}$ is much smaller than from the nearest lying layers of the PC mirrors, and it is nonzero only due to the dispersion. The increase in the SH intensity in the vicinity of $\lambda_{\omega,2}$ is caused by the uniform amplification of the pump field. The SH resonance at the short-wavelength edge of the band gap has the same origin: the strong θ dependence of the SH enhancement in this region is caused by the strong dispersion of the PS quadratic susceptibility in the vicinity of 370 nm, which is close to the energy of two-photon resonance of the direct electronic transitions E_0'/E_1 in silicon. This explains why the intensity increase at the edge of the photonic band gap is the largest at θ = 55° (Fig. 3a).

Thus, when built in the porous silicon photonic crystal, the microcavity layer gives rise to an additional SH resonance, analogous to the resonant increase in the combined density of states for the direct electronic transitions to the impurity level in the semiconductor energy gap. The nonlinear polarization is localized in the vicinity of the microcavity layer. The spectral position of the cavity mode and the radius of localization can be varied by varying the microcavity parameters.

This work was supported by the Russian Foundation for Basic Research (project nos. 00-02-04026 and 00-15-96555), the Deutsche Forschungsgemeinschaft (grant nos. 436 RUS 113/439/0 and MA 610/20-1), NATO (grant no. PST.CLG975264), and the scientific training center “Fundamental Optics and Spectroscopy” within the framework of the Federal Program “Integration.”

REFERENCES

1. M. Scalora, J. P. Dowling, C. M. Bowden, *et al.*, Phys. Rev. Lett. **73**, 1368 (1994).
2. E. Yablonovitch, Phys. Rev. Lett. **58**, 2059 (1987).
3. A. Imhof, W. Vos, R. Sprik, *et al.*, Phys. Rev. Lett. **83**, 2942 (1999).
4. C. J. Herbert and M. S. Malcuit, Opt. Lett. **18**, 1783 (1993).
5. S. John, Phys. Rev. Lett. **58**, 2486 (1987).
6. V. Berger, Phys. Rev. Lett. **81**, 4136 (1998); N. G. Broderick, G. W. Ross, H. L. Offerhaus, *et al.*, Phys. Rev. Lett. **84**, 4345 (2000).
7. S. Nakagawa, N. Yamada, N. Mikoshiba, *et al.*, Appl. Phys. Lett. **66**, 2159 (1995).
8. A. V. Balakin, V. A. Bushuev, N. I. Koroteev, *et al.*, Opt. Lett. **24**, 793 (1999).
9. L. A. Golovan’, A. M. Zheltikov, P. K. Kashkarov, *et al.*, Pis’ma Zh. Éksp. Teor. Fiz. **69**, 274 (1999) [JETP Lett. **69**, 300 (1999)].
10. V. Pellegrini, A. Tredicucci, C. Mazzoleni, *et al.*, Phys. Rev. B **52**, R14328 (1995); M. Cazzanelli and L. Pavesi, Phys. Rev. B **56**, 15264 (1997).
11. L. A. Kuzik, V. A. Yakovlev, and G. Mattei, Appl. Phys. Lett. **75**, 1830 (1999).
12. G. Mattei, A. Marucci, and V. A. Yakovlev, Mater. Sci. Eng. B **B51**, 158 (1998).
13. Yu. E. Lozovik and A. V. Klyuchnik, in *The Dielectric Function of Condensed Systems*, Ed. by L. V. Keldysh, D. A. Kirzhnitz, and A. A. Maradudin (Elsevier, Amsterdam, 1989), Chap. 5, p. 368.
14. D. E. Aspnes and A. A. Studna, Phys. Rev. B **27**, 985 (1983).
15. D. S. Bethune, J. Opt. Soc. Am. B **6**, 910 (1989).

Translated by V. Sakun